CHAPTER 103

LABORATORY EXPERIMENTS ON GENERATION OF LONG WAVES IN THE SURF ZONE

Akio Okayasu[1], Teruki Matsumoto[2] and Yasuyuki Suzuki[3]

Abstract

Laboratory experiments were performed to investigate generation of long waves in the surf zone. Amplitude of long waves generated by time-varying breaking points was found to be nearly same as that of incoming bounded long wave. The generated long waves showed phase difference with the incoming long waves. The difference of the phases reached to $3/4\ \pi$ through π at the shoreline.

1. Introduction

In order to predict the sediment transport in the nearshore area, the mechanism of generation and propagation of long period waves in the surf zone must be clarified. Long waves observed in the surf zone consist of three major components. The first component is free long wave (FLW) coming from outside of the surf zone which includes both of wave group bounded long wave (BLW) released at the breakpoint and free long waves generated by the wave maker. The second component is breakpoint forced long wave (BFLW) which is generated by moving breakpoint due to wave group. The third one is outgoing long wave which is formed by reflection of the former two components at the shoreline.

Long wave outside the surf zone can be basically explained by the mechanism proposed by Longuet-Higgins and Stewart (1962) (see *e.g.* Sato *et al.*, 1989, Nagase and Mizuguchi, 1996). Long wave generated by moving breakpoint was also theoretically investigated by Symonds *et al.* (1982), Schäffer (1993) and others. On the qualitative description of long wave sources in the surf zone, Mizuguchi (1982) wrote that the long wave coming from outside of the surf zone

---

[1] Associate Professor, Department of Civil Engineering, Yokohama National University, 79–5 Tokiwadai, Hodogaya, Yokohama 240, Japan. E-mail: okayasu@cvg.ynu.ac.jp.

[2] Tokyu Construction Co.Ltd., Tokyo, Japan.

[3] Graduate Student, Department of Civil Engineering, Yokohama National University.

was predominant among observed onshore propagating long waves in the surf zone. On the other hand, Nakamura and Katoh (1992) considered that BFLW should be predominant.

Nagase and Mizuguchi (1996) observed BFLW by putting a single packet of wave group into stable regular wave field in a wave flume. However, quantitative analysis for generation of BFLW should be difficult by the single packet experiment. Shibayama *et al.* (1992) pointed out that phase relation between wave group and long waves in the surf zone is important for suspended sediment movement due to low-frequency velocity change. Statistic analysis of phase shift also requires the measurement under usual random wave condition in the surf zone.

In the present study, generation and propagation of long waves in the surf zone are investigated on a step, 1/30, 1/20 and 1/10 uniform beaches in a flume under irregular wave conditions. Amplitude and phase variation of the long waves in the surf zone are quantitatively investigated. The experimental results are compared with a theory proposed by Mizuguchi (1995).

2. Experimental Procedures

2.1 Experimental setup and condition

The experiments were performed in a wave flume which was 17 m long and 0.5 m wide. A random wave generator with absorption control for reflected waves was equipped at one end of the flume. Beach topography were a step, 1/30, 1/20 and 1/10 uniform beaches. The step beach consisted of the first 2 m of 1/10, the next 1 m of 1/20, 6 m of flat bed and the last 2 m of 1/10 slopes. The 1/30 and 1/20 slopes had an 1 m of 1/10 slope at the toe. The beaches were made of 15-mm-thick plywood on stainless steal base.

Surface elevation and cross-shore velocity were measured by wave gages and a optic-fiber laser Doppler velocimeter (FLV). A wave gage was set 3 m onshore of the wave paddle in the offshore constant depth region. Seven (step and 1/30) or eleven (1/20 and 1/10) measuring stations were located from the offshore side of the breaking point to the shoreline. The elevation of the velocity measuring point was 1 cm from the local bottom of the slope. Figure 1 shows the setup of the flume with the step and 1/30 beaches. The x-axis was set to be onshoreward from the shoreline at the still water level.

The experiments were performed for total 14 wave conditions. Random incident waves were designed to have the Bretshneider-Mitsuyasu spectrum. The experimental conditions are listed in Table 1. In the table, h_i is the still water depth in the offshore region, h_s the still water depth on the step, $H_{1/3}$ is the significant wave height offshore, $T_{1/3}$ is the significant wave period. $H_{1/3}$ and $T_{1/3}$ were obtained by using the zero-down cross method. The "breaking point" in the table shows the mean location of wave breaking denoted by the measuring station (St.) numbers. The positions on the x-axis of the measuring stations are listed in Table 2.
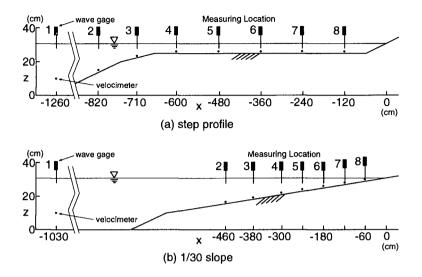
(a) step profile

(b) 1/30 slope

Figure 1: Experimental setup in wave flume

Table 1: Experimental Conditions

case	beach type	h_i (cm)	h_s (cm)	$H_{1/3}$ (cm)	$T_{1/3}$ (s)	breaking point
1–1	step	31.0	6.0	5.81	1.03	St.3
1–2				4.87	0.88	St.3
1–5		29.0	4.0	5.69	1.03	St.3
1–6				4.69	0.89	St.3
2–1	1/30	31.0	–	3.98	1.01	St.5 – St.6
2–2				3.32	0.86	St.5 – St.6
2–5		29.0	–	3.91	1.01	St.5 – St.6
2–6				3.25	0.86	St.5 – St.6
3–1	1/20	40.0	–	6.20	0.90	St.9 – St.10
3–2				7.88	1.03	St.8 – St.9
3–3				9.11	1.05	St.8 – St.9
4–1	1/10	40.0	–	6.19	0.89	St.8 – St.9
4–2				7.92	1.03	St.7 – St.8
4–3				9.28	1.03	St.6 – St.7

Table 2: Location of Measuring Stations

case	measuring location on x-axis (cm)											
	St.1	St.2	St.3	St.4	St.5	St.6	St.7	St.8	St.9	St.10	St.11	St.12
1–1 & 2	-1260	-820	-710	-600	-480	-360	-240	-120	–	–	–	–
1–5 & 6	-1240	-800	-690	-580	-460	-340	-220	-100	–	–	–	–
2–1 & 2	-1030	-460	-380	-300	-240	-180	-120	-60	–	–	–	–
2–5 & 6	-970	-400	-320	-240	-180	-120	-60	0	–	–	–	–
Series 3	-1100	-440	-400	-360	-320	-280	-240	-200	-160	-120	-80	-40
Series 4	-1260	-240	-200	-180	-160	-140	-120	-100	-80	-60	-40	-20

2.2 Data acquisition

Since only one FLV was used, the velocity measurement was repeatedly done for each measuring station with the same incident wave signal. Wave generation was started with still water condition at each time. Preparatory generation of wave was done for 600 seconds which was considered to make the wave field enough stable. Measurements of velocity and water surface elevation were conducted after this moment.

The wave profile data were sampled at the rate of 20 Hz and were stored in a digital data recorder. The velocity signal was also acquired more than 20 valid data par second. Since the time intervals of velocity records are not equal, the data were resampled every 50 ms. 300 seconds of cross-shore velocity and water surface elevation data were used for analysis.

3. Experimental Results

3.1 Extract of BFLW

Long wave components of velocity and water surface elevation of long waves were extracted by a numerical filter with the cut-off frequency of 0.25 Hz. Then the long wave components were separated into incident and reflected low frequency components by using the water surface elevation and velocity after Mizuguchi (1991).

Figure 2 shows a result of incident and reflected wave separation on the step beach for Case 1–2. In the figure, t is the time-axis, the origin of which was the start of data acquisition, and η is water surface elevation change around the mean water level. The incident component is given by the solid line and the reflected component is shown by the dotted line. The chain and the chain with 2 dots lines respectively show paths of incident and reflected free long wave calculated by the shallow water wave theory. The separation of incident and reflected long waves are found to be fairly good on the step part.

In Case 1–2, the breaking point was around St. 3 ($x = -710$ cm). By following a prominence along the incident wave path in Fig. 2, significant change
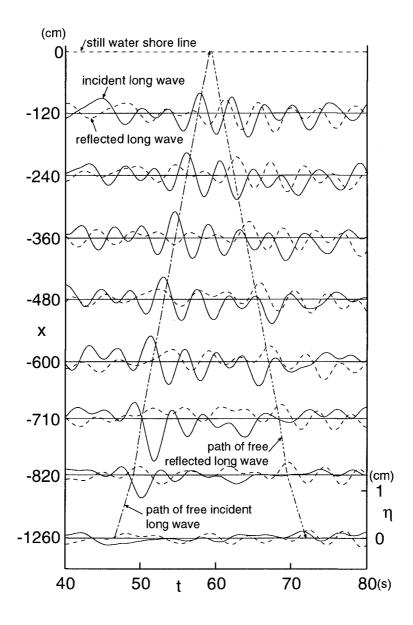
Figure 2: Incident and reflected long waves in the surf zone (chain line: path of free incident long wave, chain with 2 dots line: path of free reflected long wave)

of the amplitude and phase of the incident long wave can be seen between St. 2 and St. 4. This should be caused by generation of free long wave due to moving breakpoint.

In the present study, incoming long wave is given at a measuring station just offshore the breaking point after the separation of onshore propagating component. Onshore propagating free long wave in the surf zone can be calculated by using the shallow water wave theory from the coming long wave from the offshore-side of the boundary, the breaking point. In the present study, this calculated onshore propagating FLW is termed as "predicted free long wave (in the surf zone)". It can be considered that the deviation of observed onshore propagating FLW from this "predicted FLW" is caused by long wave generated at the breaking point. Therefore, the "measured BFLW" was obtained by "observed onshore propagating FLW" − "predicted FLW".

The dotted line in Fig. 3 shows predicted FLW for Case 1–2. This free long wave is calculated from the observed incoming long wave at St. 2. The solid line gives BFLW evaluated by subtracting the predicted FLW (dotted lines in the figure) from the observed onshore propagating long wave at each station (solid lines in Fig. 2).

The random wave field in a flume is not the same as that on the natural beach, because the seiche and multi-reflection of long waves at the flume ends as well as the unexpected free long wave generated by the wave maker affects the wave field. However, all incoming long waves from outside into the surf zone can be considered as free long waves at the breaking point. On the other hand, BFLW should be essentially the same as that on the natural beach, if the incident short wave component can be regarded as the same. Therefore, by excluding the incoming free long waves (with any origin) from the onshore propagating free long waves observed in the surf zone, the breakpoint generated long wave can be extracted with basically the same condition in the field.

The figure shows generation of relatively large long wave between St. 2 and St. 4. This generated long wave propagates onshoreward on the step as free long wave. The form of it doesn't change so much after St. 4.

3.2 Estimation of BFLW amplitude

The amplitude of BFLW was investigated quantitatively with a model proposed by Mizuguchi (1995). The displacement of water surface $\Delta\eta$ caused by onshore propagating long wave generated by the moving breakpoint is given by

$$\Delta\eta = -Ks[x_b(t) - x_{bm}]/2 \tag{1}$$

in the model. K is a constant and given by 0.194 with wave height to water depth ratio at breaking point = 0.8. s is the mean bottom slope around the breakpoint and $[x_b(t) - x_{bm}]$ the moving distance of breakpoint.

By giving $0.8\delta(1 - \kappa)h_{bm}/s$ for the moving distance of breakpoint after
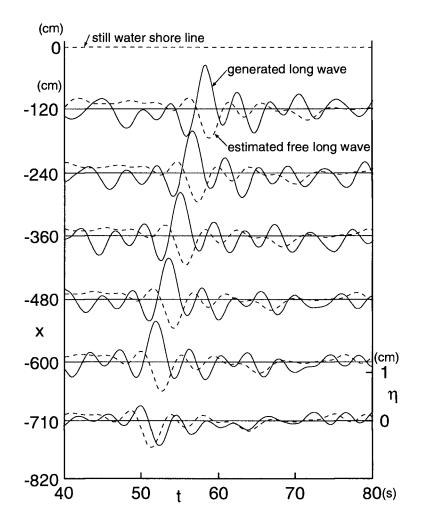
Figure 3: Predicted free long wave and generated long wave which obtained from the difference between the predicted and observed long waves

Table 3: Observed r.m.s. values of BFLW and those predicted by Mizuguchi (1995)

case	bottom slope s	breakpoint water depth h_{bm} (cm)	estimated r.m.s. value η_{crms} (cm)	measured r.m.s. value η_{mrms} (cm)	measured r.m.s. for incident wave η_{irms} (cm)
1–1		8.30	0.228	0.283	0.205
1–2	1/20	6.96	0.191	0.215	0.172
1–5		8.13	0.223	0.317	0.179
1–6		6.70	0.184	0.216	0.192
2–1		5.69	0.156	0.188	0.224
2–2	1/30	4.74	0.130	0.149	0.169
2–5		5.59	0.153	0.196	0.256
2–6		4.64	0.127	0.154	0.160
3–1		8.86	0.243	0.276	0.299
3–2	1/20	11.3	0.309	0.328	0.370
3–3		13.0	0.357	0.346	0.395
4–1		8.84	0.243	0.260	0.267
4–2	1/10	11.3	0.310	0.509	0.343
4–3		13.3	0.364	0.392	0.359

Mizuguchi (1994), Eq. 1 is obtained as

$$\Delta\eta = 0.8K\delta(1 - \kappa)h_{bm} \tag{2}$$

where δ is modulation parameter for the short waves and κ the degree of transmission of short wave grouping which are taken to be here as 0.5 and 0, respectively. h_{bm} is the mean water depth at breaking point which is approximately given by $H_{1/3}/0.7$ in the present study.

Amplitude of BFLW was calculated with above described conditions. Root-mean-square (r.m.s.) value of variation is $1/\sqrt{2}$ of the amplitude, if sinusoidal change can be assumed. Comparison between $1/\sqrt{2}$ of the calculated BFLW amplitude and observed r.m.s. value of BFLW are listed in Table 3 together with measured r.m.s. values of onshore propagating FLW (including BFLW) in the surf zone. The observed value in the table shows the mean value through the surf zone. The value 1/20 of s in Series 1 is the local bottom slope at St. 3 which was the breakpoint for the cases.

The calculated values for BFLW shown in the table are slightly smaller than the measured values. However, it can be considered that the Mizuguchi's model can predict the BFLW variation fairly well. The table also shows that the amplitude of BFLW is comparable to that of FLW coming from outside the surf zone.
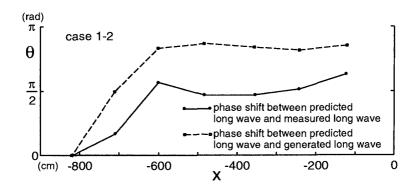
Figure 4: Phase delay of observed and generated long waves from predicted free long wave for Case 1–2

3.3 Phase shift between BFLW and incoming FLW

Cross-shore variations of phase shifts between the long wave components in the surf zone for Case 1–2 are shown in Fig. 4. θ in the figure is the phase delay from the predicted FLW (dotted line in Fig. 3) in the surf zone. The solid line in the figure gives phase delay of the observed onshore propagating long wave (solid line in Fig. 2). The broken line shows phase delay of the observed BFLW (solid line in Fig. 3).

The phase shifts were defined as mean value of Fourier components around the frequency of 0.1 Hz in spectrum analysis. The right end of the figure shows the shoreline on the beach. The phase of the observed long wave delays $\pi/2$ on the step and that of the generated long wave reaches to π. The result supports the theoretical value of phase shift π given by Mizuguchi (1995). The figure shows that the phase shifts change between St. 2 and St. 4 and quite stable on the flat bed.

Figure 5 shows phase shifts between the observed BFLW and the predicted FLW for other 3 cases on the step beach. The phase shifts are stable on the step and take values around π in all cases.

Figure 6 shows phase shifts between the observed onshore propagating long wave from the predicted FLW for Series 2, 3 and 4 which were the measurements on 1/30, 1/20 and 1/10 constant slopes. The horizontal axis in the figure is non-dimensionalized by the surf zone width x_b. The straight bold broken line in the figure shows $\theta = 0.4\pi x/|x_b|$. Although the deviation of the phase shifts near the shoreline is large, this bold broken line shows good agreement with the phase shift variations in the surf zone for all cases.

Figure 7 shows phase shifts between the observed BFLW from the predicted FLW on 1/30, 1/20 and 1/10 constant slopes. The phase shift just onshore the
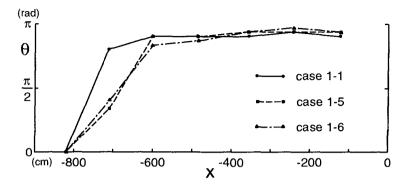
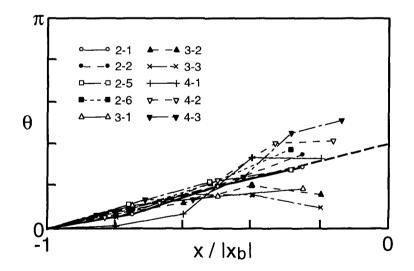Figure 5: Phase delay of generated long waves from predicted free long waves on the step beach

Figure 6: Phase delay of observed long waves from predicted long waves on the constant slope bottoms
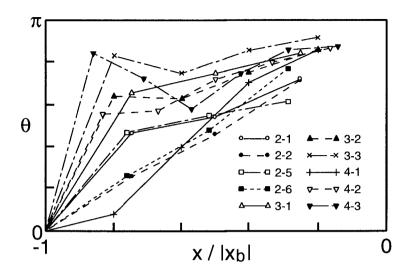
Figure 7: Phase delay of generated long waves from predicted long waves on the constant slope bottoms

breaking point takes various value. However, the value near the shoreline is within the rage of 0.6 – 0.9 π. The average is around $3/4\pi$.

As mentioned before in this section, the theoretical phase shift between BFLW and bounded long wave at the breaking point which should be transferred to free long wave in the surf zone is π (Mizuguchi, 1995). Near the breaking point, the measured values in the figure show wide variation and is far smaller than π . In the case of large short wave modulation, the generated long wave (BFLW) is relatively small near the mean breakpoint. This causes poor separation of generated long wave, then results in a large error in the phase calculation. Since the generated long wave becomes enough large, the stable phase shift close to π can be obtained near the shoreline. On the step, where the generation of BFLW is almost finished, the phase shifts show values close to π as seen in Fig. 5.

4. Calculation of BFLW by a Numerical Wave Model

It is considered that BFLW can be numerically simulated by presenting momentum flux change due to wave breaking in time and space. The concept is basically the same as Symonds et al. (1982) or Mizuguchi (1995) did in their theoretical models.

Watson et al. (1994) numerically simulated propagation and run-up of BFLW caused by a single wave group with a non-linear shallow water equation. In the
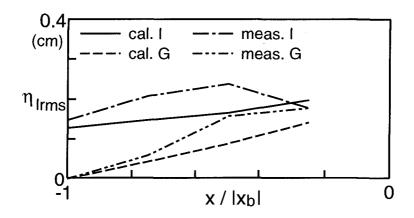
Figure 8: Comparison of r.m.s. values of calculated and measured long waves in the surf zone (Case 2-1)

present study, numerically simulated long waves in the surf zone were compared with the observed waves under random short wave conditions. Information on phase shifts can be examined with the random waves.

Boussinesq-type nonlinear dispersive wave model was used for the numerical simulation. Wave energy dissipation was expressed by a surface roller model which had been proposed by Deigaard (1989). Advantages for using the surface roller model in the simulation is: 1) Breakpoints are determined for individual short waves. Characteristics of wave groupiness can be reflected in the numerical calculation. 2) Momentum flux of surface rollers is included in the calculation. 3) Since the surface roller area is determined from the surface geometry, catching up of a wave crest to the previous wave crest can be simulated in the calculation, *etc.*

An example of the results of numerical simulations is shown in Fig. 8. Comparisons of r.m.s. values of the simulated and measured long waves for Case 2-1 are given. The solid line in the figure shows calculated onshore propagating long wave and the chain line gives measured onshore propagating long wave. The broken line is calculated BFLW and the chain with 2 dots line is measured BFLW. The calculated values at the shoreline show good agreement with measured values.

Figure 9 gives calculated and measured phase shifts between onshore propagating long wave and BFLW for Case 2-2. The solid line in the figure is calculated phase delay of onshore propagating long wave (including BFLW) from incoming long wave. The broken line is calculated phase delay of BFLW from incoming long wave. The chain line shows observed phase delay of onshore
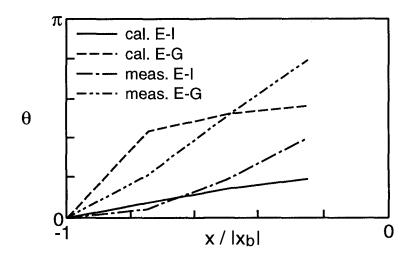
Figure 9: Comparison of phase shifts of calculated and measured long waves in the surf zone (Case 2–2)

propagating long wave and the chain with 2 dots line is observed phase delay of BFLW. Calculated phase shifts near the shoreline are slightly smaller than the observed values. However, it is considered that the numerical simulation can be used for evaluation of BFLW with phase information.

5. Conclusions

In the present study, laboratory experiments were performed for long waves observed in the surf zone under random incident wave conditions. Breakpoint forced long wave (BFLW) was evaluated from the measured cross-shore velocity and surface water elevation. Phase relation between incoming long wave and BFLW was also investigated for various wave conditions and beach topography.

The conclusions of this study are as follows:

1. With propagation of random waves onshore in a flume, long wave generated near the breaking point was observed in the surf zone. This long wave is considered to be generated by time-varying breakpoint.

2. Root-mean-square value of the generated long wave was comparable to that of incoming long wave propagating from outside of surf zone. Predicted amplitude of generated long wave calculated after Mizuguchi (1995) showed good agreement with the observed value.

3. Phase shift was found between the observed long wave in the surf zone and predicted free long wave which was calculated by using shallow water approximation. The phase delay of the onshore propagating long wave was roughly

evaluated by $\theta = 0.4\pi x/|x_b|$. Phase delay of the generated long wave from that of the incoming free long waves was around $3/4 \pi$ (for constant slopes) through π (for step-type beach) at the shoreline.

4. Boussinesq-type nonlinear dispersive wave model with the surface roller model can quantitatively simulate BFLW. The phase information can be also evaluated by the numerical model.

References

Deigaard R. (1989): Mathematical modelling of waves in the surf zone, Prog. Rep. No. 69, Inst. of Hydrodyn. and Hydraulics Eng., Tech. Univ. of Denmark, pp. 47–60.

Longuet-Higgins, M. S. and R. W. Stewart (1962): Radiation stress and mass transport in gravity waves, with application to "surf beat", J. Fluid Mech., Vol. 13, pp. 481–504.

Mizuguchi, M. (1982): A field observation of wave kinematics in the surf zone, Coastal Eng. in Japan, Vol. 25, pp. 91–107.

Mizuguchi, M. (1991): Separation of incident and reflected waves in shallow water, Proc. of Coastal Eng., JSCE, Vol. 38, pp. 31–35 (in Japanese).

Mizuguchi, M. (1995): A simple analysis of long wave generation by time-varying breakpoint, Coastal Eng. in Japan, Vol. 38, pp. 105–109.

Nagase, S. and M. Mizuguchi (1996): Laboratory experiment on long wave generation by time-varying breakpoint 25th Int. Conf. on Coastal Eng., ASCE (in press).

Nakamura, S. and K. Katoh (1992): Generation of infragravity waves in breaking process of wave group, 23rd Int. Conf. on Coastal Eng., ASCE, pp. 990–1003.

Sato S., T. Isayama and T. Shibayama (1989): Long-wave component in near-bottom velocities under random waves on a gentle slope, Coastal Eng. in Japan, Vol. 32, No. 2, pp. 149–159.

Schäffer, H. A. (1993): Infragravity waves induced by short-wave groups, J. Fluid Mech., Vol. 247, pp. 551–588.

Shibayama T., A. Okayasu and M. Kashiwagi (1992) : Long period wave and suspended sand transport in the surf zone, 23rd Int. Conf. on Coastal Eng., ASCE, pp. 2438–2449.

Symonds, G., D. A. Huntley and A. J. Bowen (1982): Two-dimensional surf beat: long wave generation by a time-varying breakpoint, , J. Geophys. Res., Vol. 87, C1, pp. 492–498.

Watson, G., T. C. D. Barnes and D. H. Peregrine (1994): The generation of low-frequency waves by a single wave group incident on a beach, 24th Int. Conf. on Coastal Eng., ASCE, pp. 776–790.